Toward a Better Understanding of the Regioselectivity of the Al(III)−Protocatechuic Acid Complexation Reaction

Erwan André, Christine Lapouge, and Jean-Paul Cornard*

LASIR, CNRS, UMR8516, Department of Chemistry, Université des Sciences et Technologies de Lille, Bâtiment C5, 59 655 Villeneuve d'Ascq Cedex, France

Received: March 18, 2008; Revised Manuscript Received: June 19, 2008

Protocatechuic acid presents two complexing sites in competition to fix metal: the carboxylic and catechol functions. Even in acidic aqueous medium, where the free ligand is fully protonated, Al(III) forms a chelate with the doubly deprotonated catechol group. To gain a better understanding of the complexation mechanism and to explain the regioselectivity of the reaction, reaction pathways involving either the catechol group or the carboxylic one have been calculated at the B3LYP/6-31G(d,p) level of theory. All the intermediate species have been identified, and both processes present the following different steps: metal attack with the coordination of Al(III) to an oxygen atom; deprotonation of hydroxyl groups; ring closure to form a chelate. Whatever the complexing site, a bidentate complex is more stable than a monodentate one. From an energetic point of view, the reaction pathway corresponding to a chelate formation with the catechol function is favored; notably the energy barrier necessary to close the ring involving the metal ion is calculated to be lower than that of carboxyl function.

1. Introduction

Humic substances (HS) are complex organic materials found ubiquitously in nature, where they play an essential role in numerous environmentally important processes.[1−3] Complexation of metal ions to humic substances would be expected to play a major role in maintaining many toxic metals in a bioavailable state in the environment. Despite the continuous investigations on humic material, the exact structures of the different HS fractions have not been well-defined. HS exhibit similar functional groups, mainly of carboxylic and phenolic types, and are characterized by their exceptional complexation capabilities toward metal ions.[4−8] The behavior of metals toward these ill-defined natural compounds is complicated because of the large number of possible interactions. In an effort to understand humic−metal interactions, some discrete ligand models (such as citric, salicylic, malic, phthalic, and benzoic acids, etc.) have been used in the study of complexation properties of humic substances.[9−14] Phenolic acids are a well-known family of natural compounds, which have as a general chemical structure an aromatic nucleus and phenolic and carboxylic functions. Phenolic acids are present in the plant kingdom, and represent a large fraction of the chemical structure of humic substances. Studies reveal that the amount of phenolic acids (e.g., caffeic, ferulic, gallic, chlorogenic, and protocatechuic acids) in HS is evaluated to be up to 35%, depending on the humus origin.[15] This class of compounds may play an important role in metal complexation by HS. Detailed investigations of humic substances have confirmed that different dihydroxyaromatic acid moieties (catechol-type groups) have an essential function as structural building blocks.[16,17] The information obtained using this type of compounds, as discrete ligand models, can be helpful in predicting the nature of the metal binding sites in HS.

Protocatechuic acid (3,4-dihydroxybenzoic acid) is commonly known as a precursor of HS[3,4,18] and has already been used as a model compound to gain a better understanding of the metal complexation reactions with HS.[19−21] This compound possesses two potential metal binding sites in competition: the carboxylic group and the catechol function (1,2-dihydroxybenzene). The implied fixing site strongly depends on the metal. Thus, for example, with regard to caffeic acid which presents the same sites in competition, Al(III) is fixed on the catecholate function while Pb(II) preferentially coordinates to the most acidic function in aqueous solution.[22,23] Recently, we showed that progressive additions of Al(III) to a protocatechuic acid solution in methanol led to the successive formation of two complexes of stoichiometry 1:1 and 2:1 (metal:ligand). By using electronic spectroscopy combined with time-dependent density functional theory (TD-DFT), it could be highlighted that the first complex corresponds to the fixing of a metal ion to the catechol function.[24] By comparison of the complex experimental spectrum with theoretical spectra calculated from several hypothetical structures, the TD-DFT methodology has proven to be a powerful tool to determine the preferential complexing site involved in the metal fixing. Nevertheless, no information about the complexation mechanism is available from the electronic spectra. The aim of this paper is to explain the regioselectivity of Al(III) complexation with protocatechuic acid (H_3PCA), to understand why the catechol function is preferred for this metal ion. To reach this goal, reaction pathways corresponding to the complexation of Al(III) with the two potential sites within the ligand have been calculated. All elementary steps involved in these mechanisms have been identified to highlight the rate-determining step governing the regioselectivity. In order to limit the number of species, and notably the hydroxy forms of Al(III), complexation reaction has been performed in aqueous solution at pH 3.5. Under such conditions only fully protonated H_3PCA ($pK_a = 4.3$)[25] and $[Al(H_2O)_6]^{3+}$ are preponderant in solution. Therefore, only these species have been taken into account in the reaction pathway calculations.

* To whom correspondence should be addressed. Telephone: +33.3.20.43.69.26. Fax: +33 0.3.20.43.67.55. E-mail: jean-paul.cornard@univ-lille1.fr.

10.1021/jp802362j CCC: $40.75
Published on Web 09/13/2008

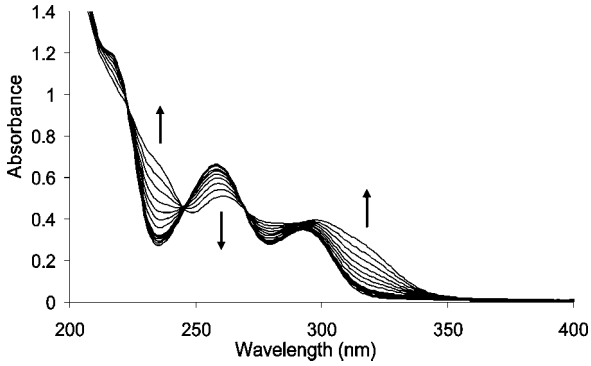

Figure 1. Evolution of UV−visible absorption spectra of protocatechuic acid with the addition of Al(III) for molar ratios varying from 0 to 10 in aqueous solution at pH 3.5.

2. Computational Details

All calculations were performed within the DFT methodology with the Gaussian 03 package.[26] Geometry optimizations were computed without symmetry constraints at the B3LYP/6-31G(d,p) level of theory;[27,28] polarization functions have been added on all the atoms to correctly take into account the intramolecular hydrogen bonds. Frequency calculations were carried out to characterize each species as minimum or as transition state, according to the number of negative eigenvalues of the Hessian matrix. The enthalpies and Gibbs free energies were calculated at 298.15 K for all the species identified in the pathways.

The enthalpies of all the stationary points of the reaction pathways have also been evaluated at the B3LYP/6-311+G(d,p) level of theory, as single points.

3. Results and Discussion

3.1. Al(III) Complexation in Acidic Medium. Al(III) complexation with H_3PCA in acidic aqueous solution has been studied by electronic absorption spectroscopy. Throughout the dosage, the pH was kept constant (pH 3.5), knowing that for this value the largely predominant species of the ligand is the completely protonated form. The different spectra were recorded on a Cary-1 (Varian) spectrophotometer with cells of 1 cm path length, at 298 K. A flow cell was used to allow successive additions of small amounts of aluminum chloride directly into the H_3PCA solution. The Al(III)/[H_3PCA] ratio was increased from 0 to 10, and the corresponding spectra are reported in Figure 1. The presence of one isosbestic point is characteristic of the coexistence of two different species in equilibrium: the free and a complexed forms. In these pH conditions, only a binding site is involved in the complex. A former study[24] has identified a complex of 1:1 stoichiometry where the metal is chelated by the fully deprotonated catechol function. It can be noted that, in such very acidic conditions, the Al(III) complexation relatively easily occurs, and that the metal is in favorable competition with the protons of the hydroxyl groups of the catechol.

3.2. Complexation Reaction Pathways. The atomic numbering used in the text is reported in Figure 2. The reaction pathways corresponding to the Al(III) complexation with the carboxylic acid function and with the catechol function with an attack on O8 and O9 have been calculated. Along these pathways, the Al atom always forms six bonds to keep its hexacoordinated environment. Along the pathways, it was impossible to highlight transition states corresponding to the departure of the various water molecules in the metal environment. Indeed, in all the tests carried out, the water molecule in departure forms one or more strong hydrogen bonds with the ligand or other close water molecules. Consequently, in the obtained structures, the reaction coordinate never corresponds to the Al−O stretching. Thus, all the steps involving a water molecule departure and bond formation are considered as a concerted mechanism occurring spontaneously, without a transition state. Thus, the only transition structures encountered along the routes correspond to deprotonation steps. For these transition state calculations, a water molecule has been introduced to assist the deprotonation. Indeed, without a water molecule, no transition state could be located. Moreover, the water-assisted deprotonation achieved via hydrogen bond formation between the leaving proton and the added water molecule partly simulates the reaction that occurs in aqueous solution. However, in order not to take into account the stabilizing interaction between the water molecule and the proton in departure, the energy of the transition state was obtained by a single point calculation where the water molecule was removed from the optimized structure. To be comparable, all the energies reported in the tables and figures correspond to a constant number of atoms. This has been done by adding the energy of an appropriate number of water molecules and/or hydronium ions to that of the considered compound. All the energies are given with respect to that of the reactants. In the different pathways the convention taken is to label "M" the different minima and "T" the transition states. The letters "a" and "c" stand for the nature of the functional group involved in the complexation: carboxylic acid and catechol, respectively. Tables 1 and 2 report the formulas, the enthalpies, and the Gibbs free energies (in the 6-31G(d,p) basis set) of all the species identified during the complexation with carboxylic and catechol functions, respectively. The reaction coordinates are also given for the different transition states. The enthalpies calculated at the 6-311+G(d,p) level are also reported in the tables, but in the following, we will first focus on results obtained in the 6-31G(d,p) basis set.

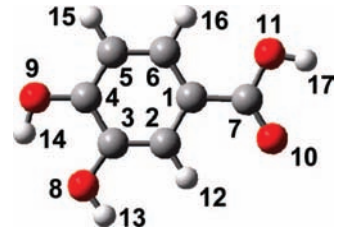

Figure 2. Atomic numbering of protocatechuic acid.

3.2.1. Chelation on the Carboxylic Acid Function. The energetic profile of this complexation mechanism as well as the structures of all the intermediates is depicted in Figure 3. The bonds corresponding to the transition state reaction coordinates are represented in broken lines. M1 represents the sum of the reactant energies of H_3PCA and $[Al(H_2O)_6]^{3+}$. The attack on O10 is exothermic and occurs spontaneously, inducing a rotation of O11H17 hydroxyl around the C7O11 bond. In this minimum (Ma2) Al is located in the ligand's plane with a Al−O10 bond length of 1.816 Å. The next step corresponds to the ring closure (C7O10AlO11) achieved with the spontaneous departure of a water molecule to keep the Al hexacoordinated environment. In the corresponding minimum (Ma3), the four-membered ring is closed and the AlO10 and AlO11 bond lengths are 1.818 and 2.130 Å, respectively. In this compound, the O11 atom forms three bonds and consequently is less bound to Al than O10. In the following transition state (Ta3) that corresponds to the hydroxyl deprotonation of the acid function, the O11H17 distance when the proton is about to leave is 1.56 Å. After the

TABLE 1: Formulas and Δ*H* and Δ*G* (in kcal·mol^{-1}) with Respect to Those of the Reactants, of Species Involved in the Reaction Pathway of the Al(III) Complexation with the Carboxylic Group of H_3PCA

		6-31G(d,p)		6-311+G(d,p)	
species	formula	Δ*H*	Δ*G*	Δ*H*	reaction coordinate
M1	$H_3PCA + [Al(H_2O)_6]^{3+}$	0.0	0.0	0.0	
Ma2	$[Al(H_2O)_5(H_3PCA)]^{3+} + H_2O$	−65.5	−65.5	−64.7	
Ma3	$[Al(H_2O)_4(H_3PCA)]^{3+} + 2H_2O$	−23.3	−33.8	−27.0	
Ta3	$[Al(H_2O)_4(H_2PCA)]^{2+}\cdots H^+ + 2H_2O$	35.3	25.6	32.3	O11···H17 = 1.56 Å
Ma4	$[Al(H_2O)_4(H_2PCA)]^{2+} + H_3O^+ + H_2O$	−141.7	−151.5	−139.2	

TABLE 2: Formulas and Δ*H* and Δ*G* (in kcal·mol^{-1}) with Respect to Those of the Reactants, of Species Involved in the Reaction Pathway of the Al(III) Complexation with the Catechol Function of H_3PCA

		6-31G(d,p)		6-311+G(d,p)	
species	formula	Δ*H*	Δ*G*	Δ*H*	reaction coordinate
M1	$H_3PCA + [Al(H_2O)_6]^{3+}$	0.0	0.0	0.0	
Mc2	$[Al(H_2O)_5(H_3PCA)]^{3+} + H_2O$	−32.7	−30.8	−32.2	
Mc2′	$[Al(H_2O)_5(H_3PCA)]^{3+} + H_2O$	−33.0	−31.3	−31.8	
Tc2	$[Al(H_2O)_5(H_2PCA)]^{2+}\cdots H^+ + H_2O$	22.4	24.2	23.4	O9···H14 = 1.60 Å
Tc2′	$[Al(H_2O)_5(H_2PCA)]^{2+}\cdots H^+ + H_2O$	23.6	25.8	25.1	O8···H13 = 1.60 Å
Mc3	$[Al(H_2O)_5(H_2PCA)]^{2+} + H_3O^+$	−148.7	−148.2	−143.3	
Mc3′	$[Al(H_2O)_5(H_2PCA)]^{2+} + H_3O^+$	−150.4	−148.8	−144.0	
Mc3″	$[Al(H_2O)_4(H_3PCA)]^{3+} + 2H_2O$	2.5	−7.1	−2.9	
Tc3a″	$[Al(H_2O)_4(H_2PCA)]^{2+}\cdots H^+ + 2H_2O$	58.6	49.0	53.4	O9···H14 = 1.57 Å
Tc3b″	$[Al(H_2O)_4(H_2PCA)]^{2+}\cdots H^+ + 2H_2O$	57.3	47.4	52.1	O8···H13 = 1.55 Å
Mc4	$[Al(H_2O)_4(H_2PCA)]^{2+} + H_3O^+ + H_2O$	−122.5	−132.7	−122.1	
Mc4′	$[Al(H_2O)_4(H_2PCA)]^{2+} + H_3O^+ + H_2O$	−121.2	−131.4	−120.8	
Tc4	$[Al(H_2O)_4(HPCA)]^{+}\cdots H^+ + H_2O + H_3O^+$	−57.5	−66.7	−56.3	O8···H13 = 1.67 Å
Tc4′	$[Al(H_2O)_4(HPCA)]^{+}\cdots H^+ + H_2O + H_3O^+$	−56.7	−66.2	−55.5	O9···H14 = 1.67 Å
Mc5	$[Al(H_2O)_4(HPCA)]^{+} + 2H_3O^+$	−155.2	−166.2	−150.2	

departure of H^+ ion, the AlO11 bond strengthens so that in the final complex (Ma4) the two AlO bonds have roughly the same lengths: 1.845 and 1.848 Å for AlO11 and AlO10, respectively.

From the energetic profile of this reaction, one can observe the formation of a monodentate complex $[Al(H_2O)_5(H_3PCA)]^{3+}$ (Ma2). This species is obtained by the simultaneous loss of a water molecule of the metal environment and the bond formation between Al and the ligand. This concerted processus is stabilizing (65.5 kcal·mol^{-1}). However, the chelate $[Al(H_2O)_4(H_2PCA)]^{2+}$ (Ma4) is 76.2 kcal·mol^{-1} more stable than the monodentate complex. The formation of the chelate from the monodentate complex necessitates crossing an energy barrier of 100.8 kcal·mol^{-1}.

3.2.2. Chelation on the Catechol Function. The reagents are the same as for the complexation on the acidic function (M1). The first step of catechol complexation is the attack of $[Al(H_2O)_6]^{3+}$ on either O9 or O8 atom (Figure 4.) In both cases this attack is spontaneous and leads to the minima Mc2 and Mc2′, respectively. In these two complexes the metal is out of the ligand plane (∼82° for Mc2 and ∼77° for Mc2′) as well as the H atom of the attacked hydroxyl group. The AlO8 and AlO9 bond lengths are 1.922 and 1.930 Å, respectively. The energy gain for M1−Mc2 (32.7 kcal·mol^{-1}) is slightly smaller than that for M1−Mc2′ (33.0 kcal·mol^{-1}). In these two structures, the intramolecular H-bond of the catechol moiety has been broken. From Mc2 and Mc2′ minima there are two ways to close the ring: either the attacked oxygen loses its hydrogen atom and then Al binds to the second hydroxyl group through

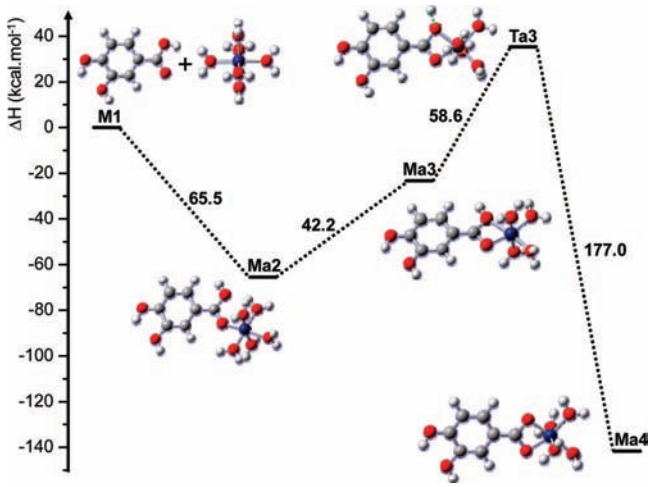

Figure 3. Energetic profile and structures of each species involved in the complexation mechanism of $[Al(H_2O)_6]^{3+}$ on the carboxylic function of protocatechuic acid. (M, minimum; T, transition state).

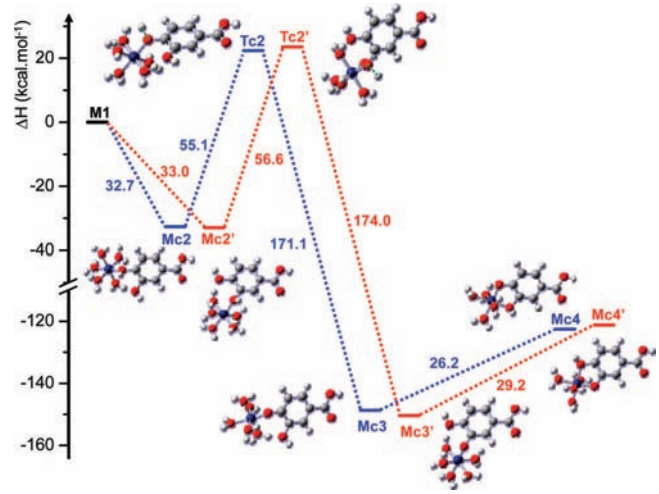

Figure 4. Energetic profile and structures of each species involved in the following steps of the complexation mechanism of $[Al(H_2O)_6]^{3+}$ on the catechol group of protocatechuic acid: metal attack, monodentate complex formation, and ring closure (way 1; M, minimum; T, transition state).

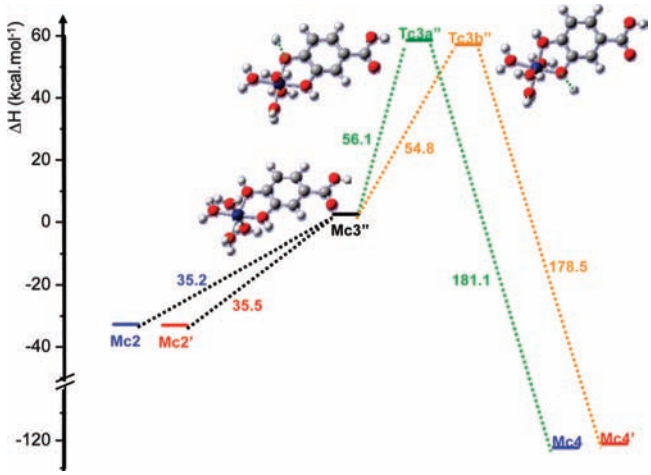

Figure 5. Energetic profile and structures of each species involved in the following steps of the complexation mechanism of $[Al(H_2O)_6]^{3+}$ on the catechol group of protocatechuic acid: formation of the fully protonated chelate (ring closure) and first deprotonation (way 2; M, minimum; T, transition state).

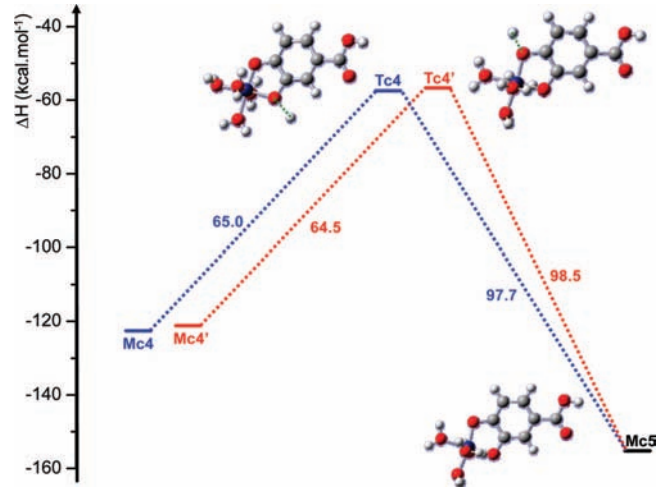

Figure 6. Energetic profile and structures of each species involved in the following steps of the complexation mechanism of $[Al(H_2O)_6]^{3+}$ on the catechol group of protocatechuic acid: second deprotonation of the catechol group and final chelate formation (M, minimum; T, transition state).

the loss of a water molecule (way 1, Figure 4), or the chelation proceeds before the deprotonation (way 2, Figure 5).

In the first way, the deprotonation of O9 and O8 gives rise, through the transition states Tc2 and Tc2′, to the minima Mc3 and Mc3′, respectively. Barrier heights of 55.1 and 56.6 kcal·mol^{-1} must be crossed to reach the transition states. The O8H13 and O9H14 reaction coordinates are identical in Tc2 and Tc2′ (1.60 Å). In the $[Al(H_2O)_5(H_2PCA)]^{2+}$ monodentate complex (Mc3) the metal atom is still out of the ligand plane (C4C3O8Al ∼ 83°), whereas in Mc3′ the C3C4O9Al dihedral angle is smaller (∼63.6°). In both complexes, the AlO bond lengths are equal to 1.746 Å, which is shorter than the value calculated for the corresponding monodentate complex on the acid function Ma2 (1.816 Å). The deprotonation completion is greatly exothermic in both cases, with an energy stabilization of 171.1 kcal·mol^{-1} for the Tc2−Mc3 step and 174.0 kcal·mol^{-1} for the Tc2′−Mc3′ one. To sum up, the monodentate complex formed via coordination with O8 lies 150.4 kcal·mol^{-1} below the reactants whereas the one with O9 lies 148.7 kcal·mol^{-1} below.The chelation occurs with the closure of the C3O8AlO9C4 five-membered ring (Mc4 and Mc4′). In these minima the metal is only slightly out of the ligand plane; C3C4O9Al ∼ 5° for both complexes. In each ring, the AlO bond lengths are not identical because of the presence of the proton on one oxygen atom. This H-atom is out of the ligand plane, on the opposite side of the metal one. To close the ring, the energy barrier to cross is higher for the pathway on O8 (29.2 kcal·mol^{-1}) than for the pathway on O9 (26.2 kcal·mol^{-1}).

In the second way, depicted in Figure 5, from Mc2 or Mc2′ the ring is directly closed to reach the same Mc3″ minimum via the departure of a water molecule. The Mc3″ minimum corresponds to a complex where Al is chelated to the fully protonated catechol function. The energy of this state is 2.5 kcal·mol^{-1} higher than the reactants. The AlO8 and AlO9 bond lengths are similar (∼1.92 Å) but not equal due to weak environmental differences. The metal is slightly out of the ligand plane (∼9°). In this complex the two oxygen atoms present three bonds and two routes can be envisaged according to the deprotonation order of O8 and O9. The water-assisted deprotonation of O9 leads to the previously determined minimum Mc4, via the transition state Tc3a″, whereas the O8 deprotonation leads to Mc4′ via Tc3b″. This second way, consisting in a direct ring closure, necessitates crossing a total energy barrier of 90.0 kcal·mol^{-1} between Mc2 and Tc3b″ for the lower value, and 91.6 kcal·mol^{-1} between Mc2′ and Tc3a″ for the higher one. As in the way 1, the deprotonation completion is exothermic (∼180 kcal·mol^{-1}) to form a monoprotonated chelate.

From Mc4 and Mc4′, the final steps are depicted in Figure 6. The last deprotonation of the catechol function leads in both cases to the final product: a chelate with the catecholate function (Mc5). This is achieved via the transition states Tc4 and Tc4′, with barrier heights of 65.0 and 64.5 kcal·mol^{-1}, respectively. The second deprotonation completion (∼98 kcal·mol^{-1}) is less exothermic than the first one. The chelate is totally planar; the AlO8 and AlO9 bond lengths (1.774 and 1.794 Å, respectively) are shorter than those calculated for the chelate on the acid group. The chelate formed with the catechol function corresponds to the lowest energy minimum of the whole pathway and lies 155.2 kcal·mol^{-1} below the reagents. As observed in the case of the acidic function, the chelate formed with the catecholate moiety is more stable than a monodentate species (Mc3 or Mc3′).

The comparison of the energetic profiles of all these routes highlights the most favored mechanism for catechol complexation. It is straightforward that the first way, with a deprotonation of one oxygen atom followed by the ring closure, is preferred. Indeed, from the common minimum Mc2 (or Mc2′), way 1 presents a barrier of 55.1 kcal·mol^{-1} (56.6 kcal·mol^{-1}) to reach the deprotonation transition state Tc2 (Tc2′), with the following step being exothermic. However, way 2 necessitates crossing a barrier of minimum value 90.0 kcal·mol^{-1} to reach a deprotonation transition state Tc3a″ or Tc3b″. Therefore, way 1 is unambiguously preferred.

In way 1 (Figure 4), the attack on the two oxygen atoms (O8 and O9) is quasi-identical from an energetic point of view, with however a slight preference for the O8 atom. Indeed the Mc2′ minimum lies 0.3 kcal·mol^{-1} below Mc2. However, the two barriers to cross to obtain the deprotonation transition state of the protonated chelate are lower for the route corresponding to an attack on O9. Indeed, there are 55.1 kcal·mol^{-1} between Mc2 and Tc2 and 56.6 kcal·mol^{-1} between Mc2′ and Tc2′ on one hand; on the other hand, the barrier heights are 91.2 kcal·mol^{-1} between Mc3 and Tc4 and 93.7 kcal·mol^{-1} between Mc3′ and Tc4′. This seems to favor a complexation via a metal attack on the O9 oxygen atom. Nevertheless, these small

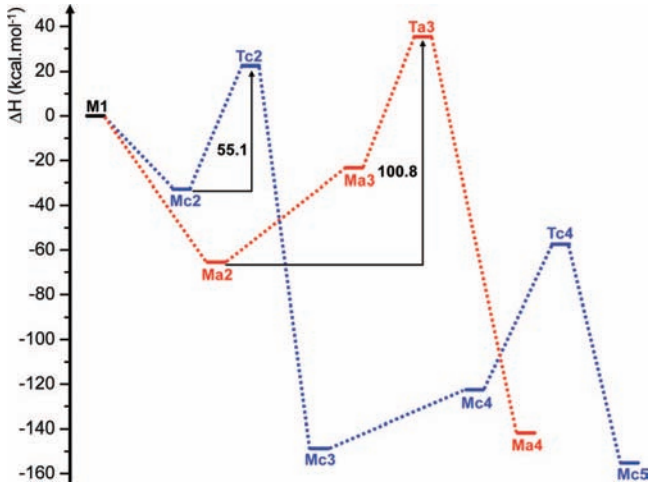

Figure 7. Comparison of the energetic profile of the mechanisms: chelation with the carboxylic group and the most probable way to the chelate formation with the catechol function (M, minimum; T, transition state).

differences in energy do not permit total exclusion of one of these routes and both mechanisms consisting in an attack on O8 or O9 should coexist.

3.2.3. Comparison of the Energetic Profiles Calculated for the Two Chelating Sites. A better understanding of the regioselectivity of the complexation reaction of Al(III) could be obtained with a comparison of the reaction pathways leading to a chelate with the carboxylic and catechol functions. For the latter, to facilitate the comparison, only the route involving the metal attack on the O9 atom will be considered, knowing that the same conclusions could be drawn by considering the other route of way 1 (attack on O8).

The two pathways as well as the energy barriers of the two complexation reactions are depicted in Figure 7. In both cases, the energy-demanding steps are the deprotonations and the ring closure.

In a first step, the comparison of the energy involved in the metal attack shows that this stage is favorable to the carboxylic complexation; Ma2 is lower by 32.8 kcal·mol^{-1} than Mc2. However, the following steps are endothermic and the energy increase is much lower in the case of complexation on catechol (55.1 kcal·mol^{-1}) than on the carboxylic group (100.8 kcal·mol^{-1}). This undoubtedly implies that the Al(III) complexation occurs with the catechol group. Moreover, it can be pointed out that the barrier corresponding to the ring closure followed by the deprotonation transition state for both routes (Ma2 to Ta3 and Mc3 to Tc4) is lower for the catechol function with 91.2 kcal·mol^{-1} versus 100.8 kcal·mol^{-1} for the carboxylic one. Then, the ring closure followed by the proton departure from the carboxylic group constitutes the rate-determining step for a chelate formation with this function.

It must be noted that, along this paper, only the ΔH values have been noted, but the same conclusions could be drawn if Gibbs free energies, reported in Tables 1 and 2, are considered. The barrier height of the first deprotonation of the complex on the catechol function is similar when ΔG (55.0 kcal·mol^{-1}) or ΔH (55.1 kcal·mol^{-1}) is considered. For the ring closure and the following deprotonation transition state, for both sites, the barrier height is lower by ∼10 kcal·mol^{-1} with ΔG compared to ΔH, giving a difference between the two routes that remains constant.

All the pathways have also been calculated with single point energies in the 6-311+G(d,p) basis set, and the results are reported in Tables 1 and 2. It can be seen that there are only small differences between the computed relative enthalpies in both basis sets, and particularly that the trends are the same and the shapes of the energetic profiles (not shown here) are also the same. The conclusions that can be drawn from these results are exactly the same as those proposed from calculations realized in the smaller basis set in the comparison of the energy barrier heights. In the larger basis set, the calculated barrier heights are 97.0 kcal·mol^{-1} for the complexation on acidic function, and 55.6 and 87.0 kcal·mol^{-1} for the complexation on the catechol function in the order of appearance in Figure 7. Thus, the values are very comparable to those obtained with the 6-31G(d,p) basis set.

Therefore, the improvement brought by the use of a larger basis set is not really significant and we can conclude that the 6-31G(d,p) basis set is totally adapted to the present study, insofar as it gives results comparable to those obtained in a larger one, and it is much less time-consuming, particularly for the transition states.

It is also important to note that all these calculations have been carried out in a vacuum, without taking into account the solvent effects. However, we have tried to include the solvent effects with the IEF-PCM solvation model implemented in the Gaussian package; for this, all the routes have been reconstructed from single point calculation energies, as often reported in the literature. The results obtained are totally unreliable, predicting a reaction that does not occur from a thermodynamic point of view, whereas it is clear from experiments that complexation is easily realized. This shows the necessity of optimizing the geometries with the solvent to correctly take the solvation effect into account in the reaction path. Unfortunately, not only these calculations are highly computationally costly, but above all the optimization of the transition states has not converged due to the failure to describe a suitable solvation cavity of the species involving a proton departure.

4. Conclusion

The aim of this theoretical study was to extend the mechanistic insight into the Al(III)−protocatechuic acid complexation to understand why a chelation via the catechol group is preferred to a mono- or bidentate complex formation with the carboxylic group. The reaction pathways, envisaging all the possible routes, have been calculated at the B3LYP/6-31G(d,p) level of theory, and all the intermediate species (transition states and minima) have been identified. The comparison of the two pathways corresponding to complexation on both sites shows clearly that complexation, in acidic medium, is favored with the catechol function. The results exhibit that the ring closure and proton departure leading to a chelate is the rate-determining step when the Al(III) complexation is envisaged on the carboxylic group. This work demonstrates that in acidic conditions, when the protocatechuic acid is fully protonated, the complexation occurs with the catechol group because the height of the energy barrier to cross is lower in the complexation with catechol than in the chelation with carboxylic function. Even if solvation effect could not be taken into account in the pathway calculations, the results obtained in the gas phase are in fairly good agreement with the experiments carried out in aqueous solution.

Acknowledgment. Institut du Développement et des Ressources en Informatique Scientifique (IDRIS; Orsay, France) is thankfully acknowledged for the CPU time allocation. The authors also thank the Lille University Computational Center.

References and Notes

(1) Schnitzer, M.; Khan, S. U. *Humic Substances in the Environment*; Marcel Dekker: New York, 1972.

(2) Aiken, G. R.; McKnight, D. M.; Wershaw, R. L.; MacCarthy, P. *Humic Substances in Soil, Sediment, and Water*; Wiley: New York, 1985.

(3) Stevenson, F. J. *Humus Chemistry: Genesis, Composition, Reactions*, 2nd ed.; Wiley: New York, 1994.

(4) Tipping, E. *Cation binding by Humic Substances*, 1st ed.; Cambridge University Press: Cambridge, U.K., 2002.

(5) Lubal, P.; Siroky, D.; Fetsch, D.; Havel, J. *Talanta* **1998**, *47*, 401.

(6) Garcia-Mina, J. M. *Org. Geochem.* **2006**, *37*, 1960.

(7) Christl, I.; Milne, C. J.; Kinniburgh, D. G.; Kretzschmar, R. *Environ. Sci. Technol.* **2001**, *35*, 2512.

(8) Elkins, K. M.; Nelson, D. J. *Coord. Chem. Rev.* **2002**, *228*, 205.

(9) Town, R. M.; Kipton, J.; Powell, H. *Anal. Chim. Acta* **1993**, *279*, 221.

(10) Maria, P.-C.; Gal, J.-F.; Massi, L.; Burk, P.; Tammiku-Taul, J.; Tamp, S. *Rapid Commun. Mass Spectrom.* **2005**, *19*, 568.

(11) Giannakopoulos, E.; Christoforidis, K. C.; Tsipis, A.; Jerzykiewicz, M.; Deligiannakis, Y. *J. Phys. Chem. A* **2005**, *109*, 2223.

(12) Plancque, G.; Maurice, Y.; Moulin, V.; Toulhoat, P.; Moulin, C. *Appl. Spectrosc.* **2005**, *59*, 432.

(13) Plaschke, M.; Rothe, J.; Altmaier, M.; Denecke, M. A.; Fanghanel, T. *J. Electron Spectrosc. Relat. Phenom.* **2005**, *148*, 151.

(14) Plaschke, M.; Rothe, J.; Denecke, M. A.; Fanghanel, T. *J. Electron Spectrosc. Relat. Phenom.* **2004**, *135*, 53.

(15) Lehtonen, T.; Peuravuori, J.; Pihlaja, K. *Anal. Chim. Acta* **2004**, *511*, 349.

(16) Gallet, C.; Keller, C. *Soil Biol. Biochem.* **1999**, *31*, 1151.

(17) Abbt-Braun, G.; Frimmel, F. H.; Schulten, H. R. *Water Res.* **1989**, *23*, 1579.

(18) Schnitzer, M. *Soil Sci.* **1991**, *151*, 41.

(19) Giannakopoulos, E.; Stathi, P.; Dimos, K.; Gournis, D.; Sanakis, Y.; Deligiannakis, Y. *Langmuir* **2006**, *22*, 6863.

(20) Plaschke, M.; Rothe, J.; Denecke, M. A.; Fanghanel, T. *J. Electron Spectrosc. Relat. Phenom.* **2004**, *135*, 53.

(21) Borges, F.; Guimaraes, C.; Lima, J. L. F. C.; Pinto, I.; Reis, S. *Talanta* **2005**, *66*, 670.

(22) Cornard, J. P.; Lapouge, C. *J. Phys. Chem. A* **2006**, *110*, 7159.

(23) Boilet, L.; Cornard, J. P.; Lapouge, C. *J. Phys. Chem. A* **2005**, *109*, 1952.

(24) Andre, E.; Cornard, J. P.; Lapouge, C. *Chem. Phys. Lett.* **2007**, *434*, 155.

(25) Beltran, J. L.; Sanli, N.; Fonrodona, G.; Barron, D. G.; Ozkan, B.; Barbosa, J. *Anal. Chem. Acta* **2003**, *484*, 253.

(26) Frisch, M. J.; Trucks, G. W.; Schlegel, H. B.; Scuseria, G. E.; Robb, M. A.; Cheeseman, J. R.; Montgomery, J. A., Jr.; Vreven, T.; Kudin, K. N.; Burant, J. C.; Millam, J. M.; Iyengar, S. S.; Tomasi, J.; Barone, V.; Mennucci, B.; Cossi, M.; Scalmani, G.; Rega, N.; Petersson, G. A.; Nakatsuji, H.; Hada, M.; Ehara, M.; Toyota, K.; Fukuda, R.; Hasegawa, J.; Ishida, M.; Nakajima, T.; Honda, Y.; Kitao, O.; Nakai, H.; Klene, M.; Li, X.; Knox, J. E.; Hratchian, H. P.; Cross, J. B.; Bakken, V.; Adamo, C.; Jaramillo, J.; Gomperts, R.; Stratmann, R. E.; Yazyev, O.; Austin, A. J.; Cammi, R.; Pomelli, C.; Ochterski, J. W.; Ayala, P. Y.; Morokuma, K.; Voth, G. A.; Salvador, P.; Dannenberg, J. J.; Zakrzewski, V. G.; Dapprich, S.; Daniels, A. D.; Strain, M. C.; Farkas, O.; Malick, D. K.; Rabuck, A. D.; Raghavachari, K.; Foresman, J. B.; Ortiz, J. V.; Cui, Q.; Baboul, A. G.; Clifford, S.; Cioslowski, J.; Stefanov, B. B.; Liu, G.; Liashenko, A.; Piskorz, P.; Komaromi, I.; Martin, R. L.; Fox, D. J.; Keith, T.; Al-Laham, M. A.; Peng, C. Y.; Nanayakkara, A.; Challacombe, M.; Gill, P. M. W.; Johnson, B.; Chen, W.; Wong, M. W.; Gonzalez, C.; Pople, J. A. *Gaussian 03*, Revision B.04; Gaussian Inc.: Pittsburgh, PA, 2003.

(27) Becke, A. D. *J. Chem. Phys.* **1993**, *98*, 5648.

(28) Lee, C.; Yang, W.; Parr, R. G. *Phys. Rev. B* **1988**, *37*, 785.

JP802362J